Active Hyperspectral Sensing for Border Control

T. Kääriäinen, M. Mekhrengin, T. Dönsberg
VTT Technical Research Centre of Finland, Tekniikantie 1, 02150, Espoo, Finland

ABSTRACT

There is a need for sensor technologies capable of identifying illegal border crossings through foliage. In this work, we study the use of a novel active hyperspectral sensor for remote identification of persons and vehicles through foliage. The AHS sensor is based on a continuously tunable near-infrared supercontinuum light source and a microelectromechanical Fabry-Pérot interferometer for transmission band selection. Real-time spectral detection algorithms are used to identify the targets based on the spectral content of the back-scattered light. Preliminary results are presented from both in-lab and outdoors.

Keywords: border control, supercontinuum, hyperspectral, MEMS, near-infrared, spectroscopy

1. INTRODUCTION

There is a need for sensor technologies capable of identifying illegal border crossings through partial or full foliage. To address this need, EU project Foldout develops full solution for situational awareness through foliage to improve the state of the art for border control. Part of Foldout project includes evaluation of novel sensor technologies for through foliage detection of persons.

Active hyperspectral sensor (AHS) [1-5] is capable of remote spectral reflectance measurement using a supercontinuum (SC) light as an active source. Due to differences in spectral absorption by different materials, the remotely measured spectra could be used to identify materials such as fabrics, skin and metals from vegetation. The AHS sensor can operate regardless of ambient illumination conditions, as opposed to commercially available hyperspectral sensors and cameras. The high spatial coherence of the SC light source allows very accurate illumination of the unknown object. Therefore, only a small opening is enough to transmit SC radiation on to an unknown object behind foliage.

In this work, we present the design and characterization of the AHS sensor, based on a custom SC light source and microelectromechanical (MEMS) Fabry-Pérot interferometer (FPI) [6]. The sensor is designed for the detection of illegal broder-cross activities. The sensors spectral measurement is validated against reference instrument. Demonstration tests are presented from lab and in the field.

2. ACTIVE HYPERSPECTRAL SENSOR

The operation principle and a picture of the AHS sensor is shown in Figure 1. The sensor consists of light receiver and a transmitter module. The receiver detects the light that scatters from an unknown object. The transmitter consists of a SC light source and MEMS FPI filter to select the wavelength band for transmission. This approach improves eye-safety in contrast to transmitting the total SC power and spectrally resolving the return signal.

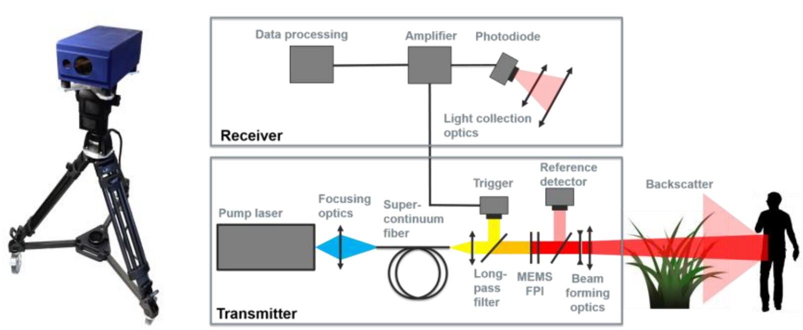

Figure 1. Operating principle of the AHS.

Electro-Optical and Infrared Systems: Technology and Applications XVIII and Electro-Optical Remote Sensing XV
edited by Duncan L. Hickman, Helge Bürsing, Gary W. Kamerman, Ove Steinvall, Proc. of SPIE Vol. 11866
118660Y · © 2021 SPIE · CCC code: 0277-786X/21/$21 · doi: 10.1117/12.2598911

In the transmitter module, SC is generated using a 1550 nm center wavelength, 100 kHz repetition rate, 1 ns pulse width, 10 kW peak power pump laser and standard telecommunication fiber. The resulting SC spectrum is shown in Figure 2a. The SC is first filtered with a longpass filter, to remove the light outside of the operating range of the MEMS FPI. The remaining light is passed through the MEMS FPI optical filter for wavelength selection. Small part of the SC radiation that passes through the MEMS FPI, is reflected towards a reference detector. The reference signal is used to correct for the high peak to peak fluctuations of the SC pulse. Furthermore, the reference signal can be used to correct for long term drifts for of the SC spectrum. Beam expander is used to achieve 8 mm beam diameter on the output.

The receiver consists of three inch diameter collection lens, that focuses the light on to an extended indium gallium arsenide (InGaAs) photodiode. The amplified signal and the reference signal is digitized with a field programmable gate array (FPGA) based data acquisition card (DAQ) RedPitaya STEMlab 125-14. The DAQ card is also used to generate a waveform ramp to sweep the transmission wavelength of the MEMS FPI. SC pulses are roughly 1 ns long, so they are spread in time by using a slow amplifier (1 Mhz). An example of reference and measurement traces are shown in Figure 2b. The data is averaged in the FPGA to produce spectra consisting of 100 channels at 10 Hz repetition rate. The sensor is mounted on a mechanical scanner (FLIR PTU-D100E) to provide spatial pointing and scanning.

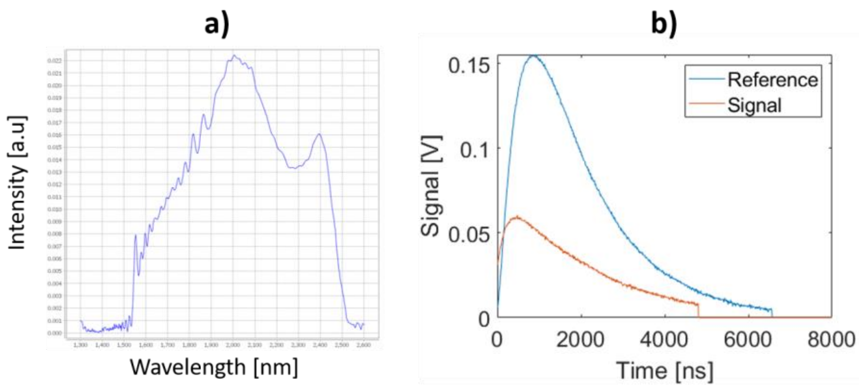

Figure 2. **a)** SC spectrum and **b)** Digitized SC pulse measured after the amplifier.

The tuning characteristics of the MEMS FPI are shown in Figure 3. The wavelength region chosen for this work covers 1900 - 2500 nm with better than 20 nm resolution across the spectrum. This region provided the best resolving spectral characteristics for different fabrics and vegetation. Furthermore, this region is an atmospheric window, having very little absorption by water vapor in the beam path. Voltage tuning of the center wavelength of the FPI is shown in Figure 3. The data from the tuning curve is used to generate a custom waveform, that results in linear wavelength sweep. The MEMS FPI used in this work has a -3 dB bandwidth of around 30 Hz, which set the limit for spectral data acquisition. The custom waveform was limited to 10 Hz spectral sweep rate.

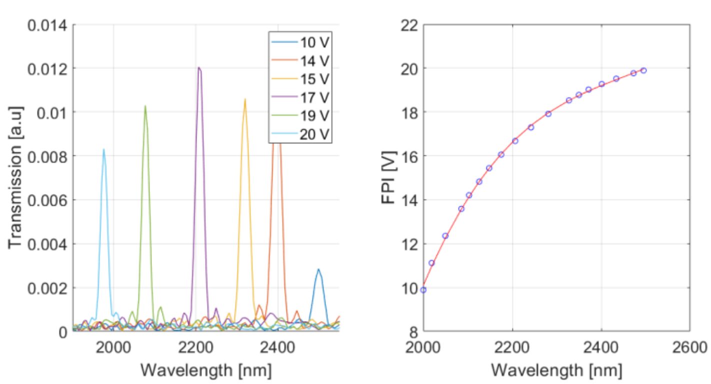

Figure 3. Tuning characteristics of the MEMS FPI.

3. RESULTS

The spectral reading of the sensor was validated by comparing the measured spectra measured with a Fourier transform infrared spectrometer (FTIR). Each measured reflection spectrum is first divided by the intensity spectrum measured from a spectral reference target (Spectralon SRT-99). Then, each spectrum is normalized by the mean value of the reflectance spectrum. An example of a comparison between AHS and FTIR is shown in Figure 4. The target in this case was a fleece jacket. Small spectral features appear more broad in the AHS data due to spectral resolution of the MEMS FPI. Nevertheless, the good agreement between AHS sensor and FTIR indicate, that spectral libraries, such as presented in [7], can be used with the AHS sensor.

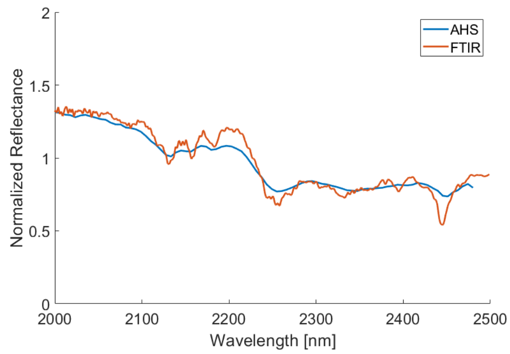

Figure 4. A comparison between AHS and FTIR.

Several reflectance spectra from different outdoor jackets, measured with the AHS sensor are shown Figure 5a. Many of the different fabrics have very similar characteristics in the spectral response, but are clearly separated from the data with high signal-to-noise ratio. In the application for border control however, it is not necessary to distinguish different fabrics. For person detection it is enough to differentiate any clothing material from the vegetation of the border area. For comparison, typical normalized reflectance of snow, soil and vegetation are shown in Figure 5b (data recreated from [8]). For each deployment site, the AHS sensor is used to measure the terrain spectra, since the spectra from the terrain varies between seasons and geography. Still, based on the comparison shown in Figure 5, significant differences can be expected between the typical clothing materials and background in the border-cross site.

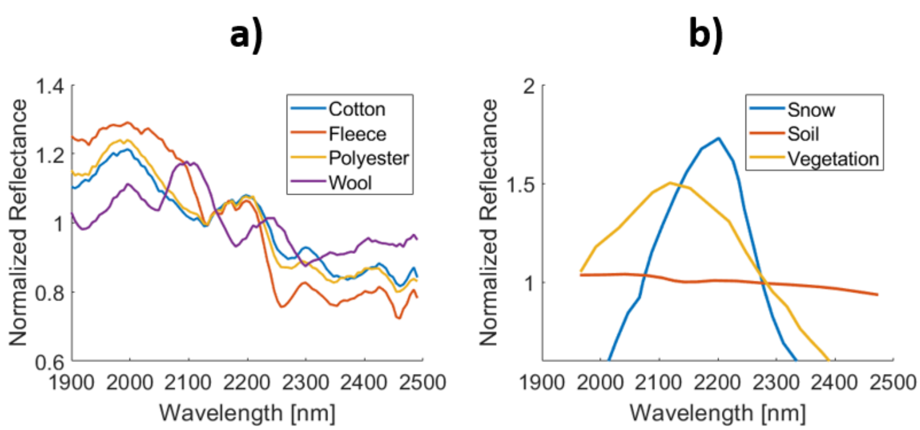

Figure 5. **a)** Selected spectra from clothes measured with AHS and **b)** typical terrain spectra recreated from [8].

The operation of the AHS was demonstrated outdoors. An example is shown in Figure 6. The sensor was placed approximately 8 m from the target area. A monochromatic camera is integrated in the system to provide visualization of the target area. The green circle indicates the measurement area for the spectral measurement. A real-time algorithm based on support vector machines were used to discriminate between the terrain spectra and different clothing materials. The surrounding vegetation was used a spectral reference for the measurement, explaining the near unity spectral response.

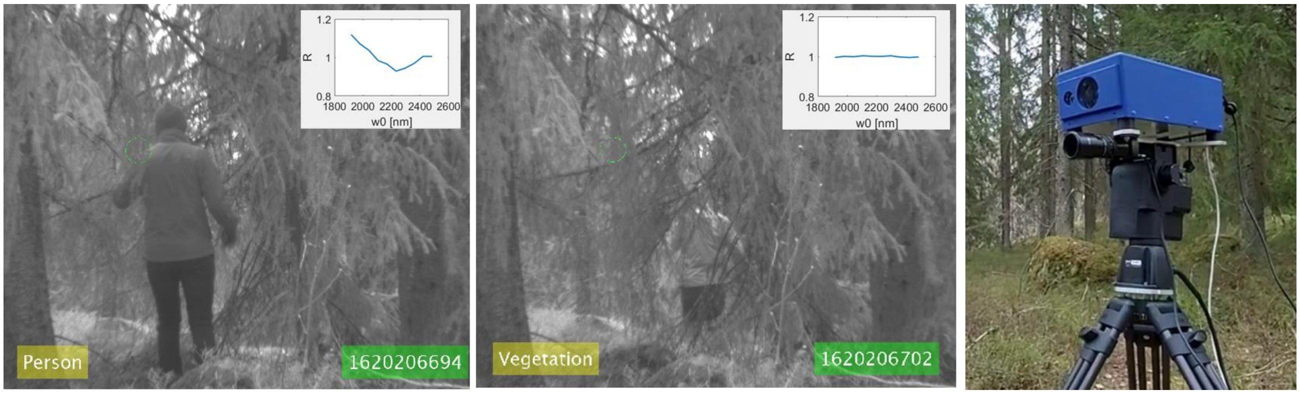

Figure 6. Field demonstration of person detection.

4. SUMMARY

An active hyperspectral sensor was developed and characterized for border control applications. The sensor was validated against FTIR and demonstrated in both lab and in the field. The wavelength region between 1900 nm - 2600 nm show promise for reliable identification of illegal border-cross activities through spectral detection of fabrics. Further work will evaluate the identification behind different levels of foliage. The proposed sensor may find alternative applications in the field of defense and security.

5. ACKNOWLEDGMENTS

The research for this work has received funding from the European Union (EU) project FOLDOUT (grant agreement n° 787021) under the EU’s Horizon 2020 Programme. https://foldout.eu/

REFERENCES

[1] Manninen, A., Kääriäinen, T., Parviainen, T., Buchter, S., Heiliö, M. and Laurila, T., “Long distance active hyperspectral sensing using high-power near-infrared supercontinuum light source,” Opt. Express 22(6), 7172-7177 (2014).

[2] Kääriäinen, T., Jaanson, P., Vaigu, A., Mannila, R., & Manninen, A. Active hyperspectral sensor based on MEMS Fabry-Pérot interferometer. Sensors, 19(9), 2192 (2019).

[3] Jaanson, P., Vaigu, A., Kääriäinen, T., Mannila, R., Lehtomäki, V., & Manninen, A., ”A continuously tunable NIR laser and its applications in material classification,” Proc. SPIE 10791, 1079107 (2018).

[4] Hakala, T., Suomalainen, J., Kaasalainen, S. and Chen, Y., “Full waveform hyperspectral LiDAR for terrestrial laser scanning,” Opt. Express 20, 7119-7127 (2012).

[5] Kilgus, J., Duswald, K., Langer, G. and Brandstetter, M.,. Mid-infrared standoff spectroscopy using a supercontinuum laser with compact Fabry–Pérot filter spectrometers. Appl. Spectrosc. 72(4), 634-642 (2018).

[6] Antila, J., Miranto, A., Mäkynen, J., Laamanen, M., Rissanen, A., Blomberg, M., Saari, H. and Malinen, J., “MEMS and piezo actuator-based Fabry-Perot interferometer technologies and applications at VTT,” Proc. SPIE 7680, 76800U (2010).

[7] Burke, M., Dawson, C., Allen, C.S., Brum, J., Roberts, J. and Krekeler, M.P., “Reflective spectroscopy investigations of clothing items to support law enforcement, search and rescue, and war crime investigations, “ Forensic sci. int. 304, 109945 (2019).

[8] Dong, Chunyu. "Remote sensing, hydrological modeling and in situ observations in snow cover research: A review." J. Hydrol. 561, 573-583 (2018).